



OPEN Neurotoxic effects of rotenone and deltamethrin prolonged exposure on adult zebrafish

Jacopo Grisotto¹, Shima Tavakolian Haghghi¹, Atena Poor Sasan¹, Serena Pedron², Matteo Brunelli², Ugo Moretti¹ & Giovanna Paolone¹

The presence of pesticides in aquatic ecosystems has become an increasing concern. Contamination of ground and surface water results from substances escaping wastewater treatment plants (WWTP) and leaching from soil. Pesticides pose a significant threat to the aquatic environment, as even trace concentrations can damage the central nervous systems (CNS) of animals and humans. Rotenone (ROT), an electron transport chain inhibitor, causes selective dopaminergic (DA) degeneration, while deltamethrin (DM), a widely used type II pyrethroid insecticide, is known for its neurotoxic effect. We assessed the impact of chronic exposure to ROT (2 µg/L, 4 weeks) and DM (1 and 2.5 µg/L, 15 days) on the central nervous system of adult zebrafish. TUNEL assay analysis ($n=15$ in total) revealed both pesticides triggered cell death in different brain regions of fish, including areas involved in sensory, motor, and cognitive processes. DM additionally affected regions associated with complex behaviors such as learning, memory, and decision-making. Immunohistological analyses ($n=12$ in total) showed loss of DA neurons in the areas involved in the motor control of animals exposed to both pesticides. These neurotoxic effects were further supported by behavioral changes ($n=38$ in total) in the Novel Tank Test (NTT), indicating alterations in movement and anxiety-like behavior. Our findings confirm that chronic sub-threshold exposure to chemicals present in environmental waters causes significant damage to cerebral tissue, leading to apoptosis and behavioral alterations.

Pesticides are of particular concern as persistent organic pollutants, exerting long-lasting effects on water and sediment quality while exhibiting high degrees of bioaccumulation in fatty tissues of aquatic organisms¹.

Despite their environmental risks, pesticides remain essential in agriculture, effectively controlling pests, diseases, and weeds to ensure high-quality crop production and minimize harvest losses². However, their widespread use has led to increased global consumption, and their application in agriculture contributes to environmental water contamination. Considering strictly the Italian territory, traces of pesticides were found in 1012 surface water and 595 groundwater monitoring points in 2020. This widespread presence highlights the persistent and worsening issue of pesticide pollution, as well as the need for meticulous management and continuous monitoring³. These chemicals contaminate water bodies through multiple pathways, including subsurface drainage, leaching, runoff, spray drift, and discharge from wastewater treatment plants (WWTPs)⁴. In aquatic systems, pesticides are absorbed by organic matter, which can be bioaccumulated and magnified in aquatic organisms, subsequently entering the food chain⁵⁻⁷. The continuous presence of these chemicals in water bodies, along with their co-occurrence with other emerging contaminants, poses a risk to both humans and ecosystems due to chronic exposure to low concentrations and potential synergistic effects⁸.

Previous studies have shown that chronic, low-level exposure to pesticides such as those targeting mitochondrial function and acting as insecticides leads to several neurodegenerative disorders, such as Parkinson's disease (PD), Alzheimer's disease (AD), and amyotrophic lateral sclerosis (ALS) through the neurotoxic mechanism of action⁹. Indeed, mitochondrial complex I inhibitors induce oxidative stress and impair mitochondrial energy production, while pyrethroids and organochlorinated chemicals affect sodium channels on the neuronal membrane, acting as CNS stimulants and inducing neuroinflammation and apoptosis¹⁰.

Rotenone (ROT), a naturally occurring, plant-derived pesticide extracted from the roots of several plants of *Derris*, *Lonchocarpus*, *Tephrosia*, and *Mundulea* species¹¹, is extensively used as an insecticide in vegetable gardens and to manage invasive or excessive fish populations in lakes and reservoirs^{12,13}. ROT is a highly lipophilic mitochondrial complex I inhibitor that rapidly crosses the blood-brain barrier, leading to neuronal damage^{14,15}. Complex I enzyme is a key protein for energy production in mitochondria, and its inhibition

¹Pharmacology section, Department of Diagnostics and Public Health, University of Verona, Verona, Italy.

²Pathology section, Department of Diagnostics and Public Health, University of Verona, Verona, Italy. ✉email: giovanna.paolone@univr.it

contributes to the pathogenesis of PD⁹. Many studies revealed that rotenone administration in rodents leads to PD-like symptoms, including DA neuron loss, α -synuclein aggregation, and reduced locomotion¹⁶. Similarly, chronic low-dose ROT treatment induces both motor and non-motor symptoms associated with PD in adult zebrafish, related to downregulation of tyrosine hydroxylase (TH)¹⁷, an essential precursor in the synthesis of catecholamines, including DA, epinephrine, and norepinephrine¹⁸.

Deltamethrin (DM) is a synthetic type II pyrethroid insecticide, introduced as a substitute for organochlorine and organophosphate pesticides also widely used in pest control. Although it is considered less harmful to the environment and non-target organisms than other insecticides, evidence suggests it also exhibits neurotoxic effects in zebrafish^{20,21}, furthermore, because of its extended half-life and low water solubility, DM residues persist in various environmental matrices, including water, air, sediment, plants, and animals^{22,23}. While the acute effects of DM exposure in fish are well-documented, its long-term impact under chronic exposure remains less explored²¹. DM impairs muscle function, suppresses reflexes, and induces severe neurological symptoms²⁴ mainly by binding to multiple ion channel families, mostly voltage-gated sodium channels (VGSC) and voltage-gated calcium channels (VGCC), ultimately disrupting neuronal signaling²⁵. Other investigations revealed that DM induced DNA fragmentation in rats' brains and exhibited irregular cell damage, with condensed and pyknotic nuclei, disrupted cell membranes, and nuclear shrinkage alongside neuronal cell swelling in the cortex and hippocampus regions. These histological alterations are likely due to the heightened oxidative stress caused by DM²⁶.

For both pesticides, the concentrations tested are within the range of values found in surface waters^{27,28}; DM: below 24 $\mu\text{g/L}$ ^{29–31}.

Zebrafish (*Danio rerio*) is a valuable vertebrate model in biomedical research employed across many scientific disciplines.

Approximately 70–80% of zebrafish genes share homology with the human genome, furthermore, although mammals and zebrafish brains develop differently (by eversion rather than inversion), primary structural and neurotransmitter systems including DA connections of the CNS, are maintained providing the zebrafish model with face, construct and predictivity validity for studying neurotoxicity^{19,32}. In the present study, we investigated ROT and DM-induced behavioral alterations and neurotoxicity at environmentally relevant concentrations found in aquatic ecosystems. Neurotoxicity was assessed in adult zebrafish, allowing us to study alterations in fully-developed brain regions associated with attention (diencephalon), learning and memory (telencephalon), visual system (optic tectum), and locomotion (cerebellum)^{33,34}. In the novel tank test, locomotor and stress-related behavioral endpoints provided valuable insights into the ethological implications of the histological alterations observed. Modifications within the diencephalon were closely associated with motor impairments, as the posterior tuberculum plays a central role in dopaminergic neuromodulation and the regulation of movement³⁵. Conversely, stress-related behaviors were associated with activation of the hypothalamic-pituitary-interrenal (HPI) axis, primarily involving the hypothalamus and the preoptic area^{36–39}.

Materials and methods

Animals

A total number of 40 AB-strain zebrafish were obtained through in-house breeding in the Interdepartmental Centre for Experimental Research (CIRSAL) at the University of Verona. Adult zebrafish (7–8 months old) were bred in a recirculating water system at 28 ± 1 °C and kept on a 14-hour light/10-hour dark cycle.

One week before exposure, fish were divided into four mixed-sex cohorts. They were then removed from the recirculating water system and placed in a thermostatic cabinet with a constantly maintained temperature and light/dark cycle. During the study, fish were fed four times daily with live food (*Artemia sp.*) and dry food (dry/live/live/dry). After a week of acclimation, behavioral tests were conducted to establish baseline levels of locomotion and anxiety-like behavior.

All animal care and experimental procedures are reported in compliance with the ARRIVE guidelines and were conducted in accordance with the European Union regulations, and the Directive 2010/63/EU. The study was approved by the ethical committee (OPBA) of the University of Verona and by the Ministry of Health (authorization n. 887/2023-PR).

Chemicals and exposure procedures

Fish were randomly assigned to each treatment. The vehicle control group was exposed to system water, while the treated fish were exposed to rotenone (ROT) 2 $\mu\text{g/L}$ for 4 weeks, or to deltamethrin (DM) 1.0–2.5 $\mu\text{g/L}$ for 15 days. The duration mismatch is due to the different modes of action of the two pesticides. DM is characterized by faster neurotoxicity induction compared to ROT^{17,21}. In line with the guiding principles for more ethical use of animals in scientific research (3Rs, Replacement, Reduction, and Refinement), one vehicle-exposed group was generated and exploited as a control for both ROT and DM treatments. Ethanol was used as a solvent, reaching a final concentration of 0.0004%. Water pH and conductivity were monitored daily.

Euthanasia and fixation

Following behavioral testing, the zebrafish were anesthetized and subsequently euthanized by hypothermal shock followed by decapitation. The vehicle group was sacrificed at the end of the study. Each fish was transferred to a beaker containing ice water, maintained at a constant temperature below 2 °C, and kept in ice for 1 min after cessation of vital signs (opercular movement, righting equilibrium, and heartbeat). An incision was made ventrally from the anal pore to the base of the pectoral fin to allow the fixative solution to penetrate the internal organs⁴⁰. The fish were then rapidly transferred to 10% formaldehyde (FM0622, Mondial s.n.c.) and kept at 4 °C for 24 h for tissue fixation.

Tissue processing

Following fixation, tissue was rinsed in 100% ethanol (EtOH, Cat. No. A0145, Diapath) and placed in an automatic Leica processor (Histocore Peloris 3, Leica Biosystems GmbH) for dehydration, clarification and infiltration at 37 °C. The dehydration process involved five ethanol washes: one in 50% EtOH and four in 100% EtOH, 30 min each. Clarification was performed with two 90-minute washes in xylene (Cat. No. 3410/20, Histo-Line laboratories srl), followed by infiltration with two 90-minute washes in liquid paraffin (Cat. No. 39601006 Leica Biosystems GmbH). The tissue was then paraffin-embedded, dipped into a decalcifying solution (Cat. No. 05-M03005 BioOptica) then cut into 5 µm thick sections using a manual rotary microtome (Cat. No. M2258 Histo-Line laboratories srl). The sections were straightened out in a warm water bath (Cat. No. WB 2800 Histo-Line laboratories srl) and then placed on adhesive glass slides (10354365 Fisher Scientific srl). Fish were sectioned in a sagittal orientation, and the cerebral regions were identified using the Adult Zebrafish Brain Atlas (AZBA)⁴¹. Tissue sections were harvested from sagittal AZBA coordinates 250 to 420, those selected for TUNEL and TH staining were from the medial portions of both hemispheres, corresponding to AZBA coordinates 320 to 350. The medial portions offer an optimal representation of the major brain structures such as telencephalon, diencephalon, optic tectum, cerebellum, and olfactory bulbs, additionally, DA neurons are organized in clusters within the medial portion of the diencephalic region.

TUNEL assay

The Terminal Deoxynucleotidyl Transferase-Mediated dUTP Nick End Labeling (TUNEL) assay was conducted on tissue sections with a commercial kit (Cat. No. C10618, Thermo Fisher Scientific Inc.) to quantify the effect of chronic pesticide exposure on cellular apoptosis. Adult zebrafish exposed to ROT and DM were euthanized, fixated and tissue sliced to obtain sagittal sections of the CNS. Medial brain sections were selected, including telencephalon, diencephalon, optic tectum, and cerebellum of both hemispheres. After deparaffinization and rehydration, tissue sections were post-fixed with 10% buffered formaldehyde, permeabilized with Proteinase K, and thoroughly washed in PBS. DNA strand breaks were induced by treating two replicates of one sample belonging to the Vehicle group with DNase I to serve as positive control. The slides were then incubated with a TdT reaction mixture to label the DNA strand breaks, followed by incubation with the TUNEL reaction cocktail. After one wash in PBS, tissues were counterstained with DAPI to visualize all nuclei. Additionally, selected slides were stained with anti-TH antibody. Briefly, after overnight incubation with 1:1000 anti-TH antibody (rabbit polyclonal, Cat No. GTX102424, GeneTex, Inc), slides were washed with PBS and incubated for one hour with AlexaFluor 488 goat anti-rabbit secondary antibody (1:1000, Cat. No. A-11034, Life Technologies Europe BV). After a 5-minute wash in PBS, sections were mounted with fluoromount (Cat. No. K048, Diagnostic BioSystems), covered with a coverslip, and conserved at +4° until analysis. Imaging was conducted with a Leica microscope (*Thunder Imager Tissue*). DAPI and TUNEL-positive cells were quantified with ImageJ software. The Apoptotic Indexes were calculated as the ratio between the number of TUNEL-positive cells and the total number of DAPI-stained nuclei. We used the obtained data to calculate the Apoptotic Index as follows:

$$\text{Apoptotic Index} = \frac{\text{Number of TUNEL - positive cells}}{\text{Total number of DAPI - stained nuclei}} \times 100\%$$

Immunohistochemistry

Chronic exposure to ROT reduces brain DA levels¹⁷, and this reduction could be associated with neuronal death. We performed TH immunohistochemistry on zebrafish brain slices to assess the extent and localization of DA neuronal death. Prior to immunohistochemical processing, the zebrafish slices were dewaxed and hydrated through a series of 3-minute washes: two in xylene, one in a 1:1 mixture of xylene and ethanol, two in 100% ethanol, followed by washes in 95%, 70%, and 50% ethanol, and concluding with 5-minutes rehydration in distilled water (deparaffinization in xylene and then rehydration through a descending gradient of ethanol). Antigen retrieval for tyrosine hydroxylase staining was performed using citrate buffer (pH 6.0) for 15 minutes at 95°C. After cooling to room temperature for 10 minutes, the slices were washed twice in Triton X-100 (0.3% in PBS; Cat. No. T8787, Merck) for 5 minutes then incubated with 1% bovine serum albumin and 10% goat serum for 1 hour. Sections were incubated overnight at 4 °C in a humidified chamber with a primary antibody specific for tyrosine hydroxylase (rabbit polyclonal, Cat No. GTX102424, GeneTex, Inc) at a dilution of 1:1000. Following two 5-minute washes in 0.3% Triton X-100 and inactivation of endogenous peroxidases with 0.3% H₂O₂ for 15 minutes, tissue slices were incubated with the biotinylated goat anti-rabbit secondary antibody (Cat. No. 65-6140, Thermo Fisher Scientific Inc.) for 1 hour at room temperature. After 2 washes in PBS, slides were incubated with ABC reagent (Cat. No. 32020, ThermoFisher Scientific) for 30 minutes. DAB (3,3'-diaminobenzidine, Cat. No. 1029240001, Merck) chromogen was applied for 10 min, followed by a 5-minute wash with PBS. The tissues were then counterstained with hematoxylin (1:20, Cat. No. C0302, Diapath spa), mounted with Entellan (Cat. No. 1.07960, Merck KGaA), covered with coverslips (Cat. No. BPD009, RS France), and dried at room temperature for 24 h.

Referring to the AZBA⁴¹, two sections per animal were selected, and TH-immunoreactive (TH-ir) neurons were examined in the olfactory bulb, preoptic area, preteectum, posterior tuberculum, and hypothalamus using a Leica brightfield microscope (Leica DM2000 LED). Images were then analyzed with ImageJ software.

Behavioral testing

Prior to behavioral testing, the fish were acclimated to handling procedures through daily transfers to a new tank using a net. During the exposure, the water was completely replaced every 24 h. Behavioral trials were performed at baseline and at the end of the treatment. The animals were moved from the ventilated cabinet to the experimental table at least one hour before starting the behavioral tests.

Novel tank test

Behavioral assessments of zebrafish were conducted 24 h after the end of the chronic pesticide exposure. The novel tank test was conducted to investigate impacts on locomotion and stress-related behaviors. Locomotion was quantified by measuring the total distance traveled by the zebrafish during the test, providing a clear indication of their swimming proficiency and overall activity levels. Additionally, the absolute turn angle was analyzed as both a measure of locomotion activity and an indicator of stress behavior. Increases in this parameter correlate with erratic swimming, a complex behavior characterized by sudden directional shifts and frequent, rapid darting. After the acclimation period, fish were individually placed in a trapezoidal tank (19 cm width at the base \times 20.5 width at the water surface \times 8 cm height) filled three-quarters with system water. The movements of the animals were recorded with a Nilox MiniUp camera for 10 min and then remotely analyzed via AnyMaze software. Tanks were ideally divided into three horizontal sections, (top, medium, and bottom). The parameters analyzed included duration of swimming at high speed (sec) (animals moved at high speed when the movements exceeded 2 cm/s), distance moved (cm), absolute turn angle (deg), number of entries (n), latency to enter (sec), and time spent in the upper zone (sec).

Statistical analysis

Data were screened for outliers through the ROUT method and subsequently excluded. The normal distribution of data was assessed before analysis. Values are expressed as mean \pm standard error of the mean (SEM). The total sample sizes in each specific endpoint were $n=38$ in behavioral trials, $n=15$ in the TUNEL, and $n=12$ in the histological analyses. The statistical significance between vehicle and ROT was assessed using Student's *t*-test, while differences between DM-exposed and vehicle groups were assessed through one-way ANOVA. Multiple comparisons between treatment groups and vehicles were carried out through the Dunnett test. All statistical calculations were performed with GraphPad Prism 10, with an α value set at 0.05. Exact *p* values are reported for significant results⁴². Hedge's *g* (in *t*-test analyses) and eta squared (η^2 , for ANOVA analyses) effect sizes were indicated as *ES*, alongside their 95% confidence interval (CI).

Results

ROT exposure

The results obtained in the present study are summarized in Table 1. Figure 1a shows the brain regions exposed to TUNEL staining in the longitudinal brain section schematically represented in Fig. 1b.

ROT exposure significantly increased the levels of apoptosis in the diencephalon (Fig. 1c; $t_{(22)}=2.994$, $p=0.0067$, $ES=1.197$, 95% CI [0.338, 2.117]), optic tectum (Fig. 1e; $t_{(27)}=3.005$, $p=0.0057$, $ES=1.101$, 95% CI [0.326, 1.922]), and cerebellum (Fig. 1g; $t_{(24)}=2.894$, $p=0.0080$, $ES=1.113$, 95% CI [0.296, 1.982]). The proportion of TUNEL-positive cells in the diencephalon and optic tectum of exposed animals reached similar magnitudes, $62.68\% \pm 3.75$ and $51.03\% \pm 7.15$, respectively. Although the cerebellum of exposed brains showed significantly higher apoptotic activity than the vehicle group ($p=0.0080$), the mean apoptotic index value remained moderate at $17.52\% \pm 3.33$.

Telencephalon (Fig. 1d; $t_{(31)}=1.370$, $p=0.1806$) and olfactory bulb (Fig. 1f; $t_{(21)}=0.5898$, $p=0.5616$) regions showed lower apoptosis, with no statistically significant changes compared to vehicle.

DM exposure

As shown in Fig. 2, DM induced significant apoptosis in the brain regions indicated in Fig. 2a of the longitudinal brain section schematically represented in Fig. 1b. In the diencephalon (Fig. 2c, $F_{(2, 40)}=12.77$, $p<0.0001$, $ES=0.390$, 95% CI [0.143, 0.585]), telencephalon (Fig. 2d, $F_{(2, 49)}=9.150$, $p=0.0004$, $ES=0.272$, 95% CI [0.083,

| Group | | Rot 2.0 | DM 1.0 | DM 2.5 |
|----------------------------------|------------------------------------|---------|--------|--------|
| Increase in TUNEL-positive cells | Diencephalon | ++ | ++ | ++++ |
| | Telencephalon | ns | ++ | +++ |
| | Optic tectum | ++ | +++ | ns |
| | Olfactory bulb | ns | + | ++ |
| | Cerebellum | ++ | ns | ++ |
| Decrease in TH-ir cells | Posterior tuberculum | + | ns | + |
| | Posterior hypothalamus | ++ | ns | + |
| | Preoptic area | ns | ns | + |
| | Olfactory bulb | ns | ns | ns |
| | Pretectum | ns | ++ | ns |
| Novel tank test | Duration of swimming at high speed | + | ns | ++ |
| | Absolute turn angle | ns | ns | + |
| | Distance moved | ns | ns | ns |
| | Latency to enter the top | + | ns | ns |
| | Number of entries to the top zone | ns | ns | ns |
| | Time in the top zone | ns | ns | ns |

Table 1. Result summary. “ns” non-significant, “+” $p \leq 0.05$, “++” $p \leq 0.01$, “+++” $p \leq 0.001$, “++++” $p \leq 0.0001$.

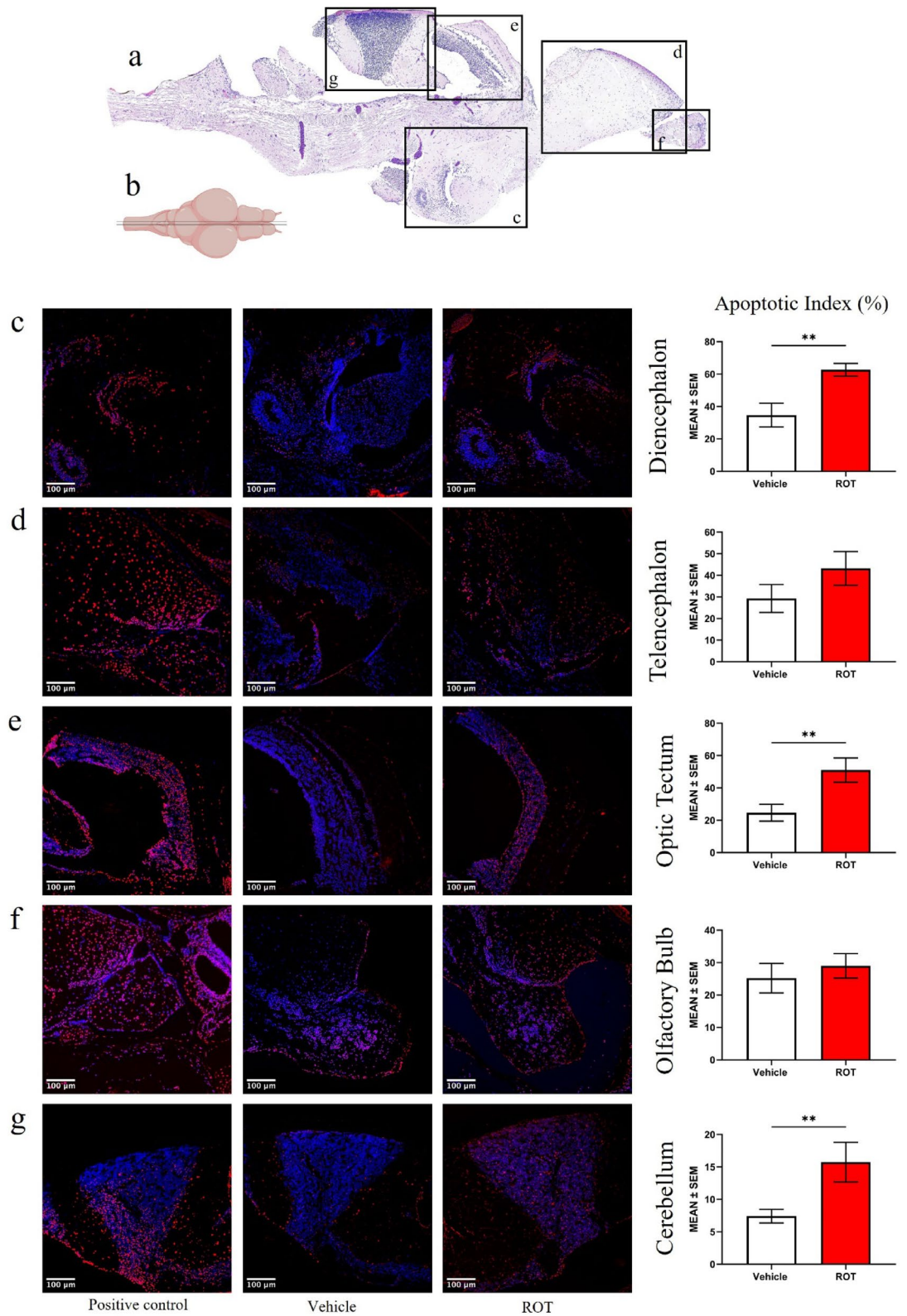


Fig. 1. Exposure to 2.0 µg/L ROT induced significant apoptosis in selected brain regions. Hematoxylin and eosin staining highlight the brain regions where the apoptotic index was assessed via TUNEL staining (a). Schematic representation of zebrafish brain in dorsal view (b). Representative images of the diencephalon, telencephalon, optic tectum, olfactory bulb, and cerebellum (c-g). Nuclei are marked by DAPI (blue). Apoptotic cells are stained with TUNEL (red). From left to right, the pictures refer to slices of the positive control (tissue slices of vehicle groups treated with DNase I to induce double-strand DNA breaks), vehicle, and ROT-treated. On the right, data are expressed as a comparison of Apoptotic Indexes between ROT and vehicle groups. Statistical analysis was performed with Student’s t-test, * $p < 0.05$, ** $p < 0.01$.

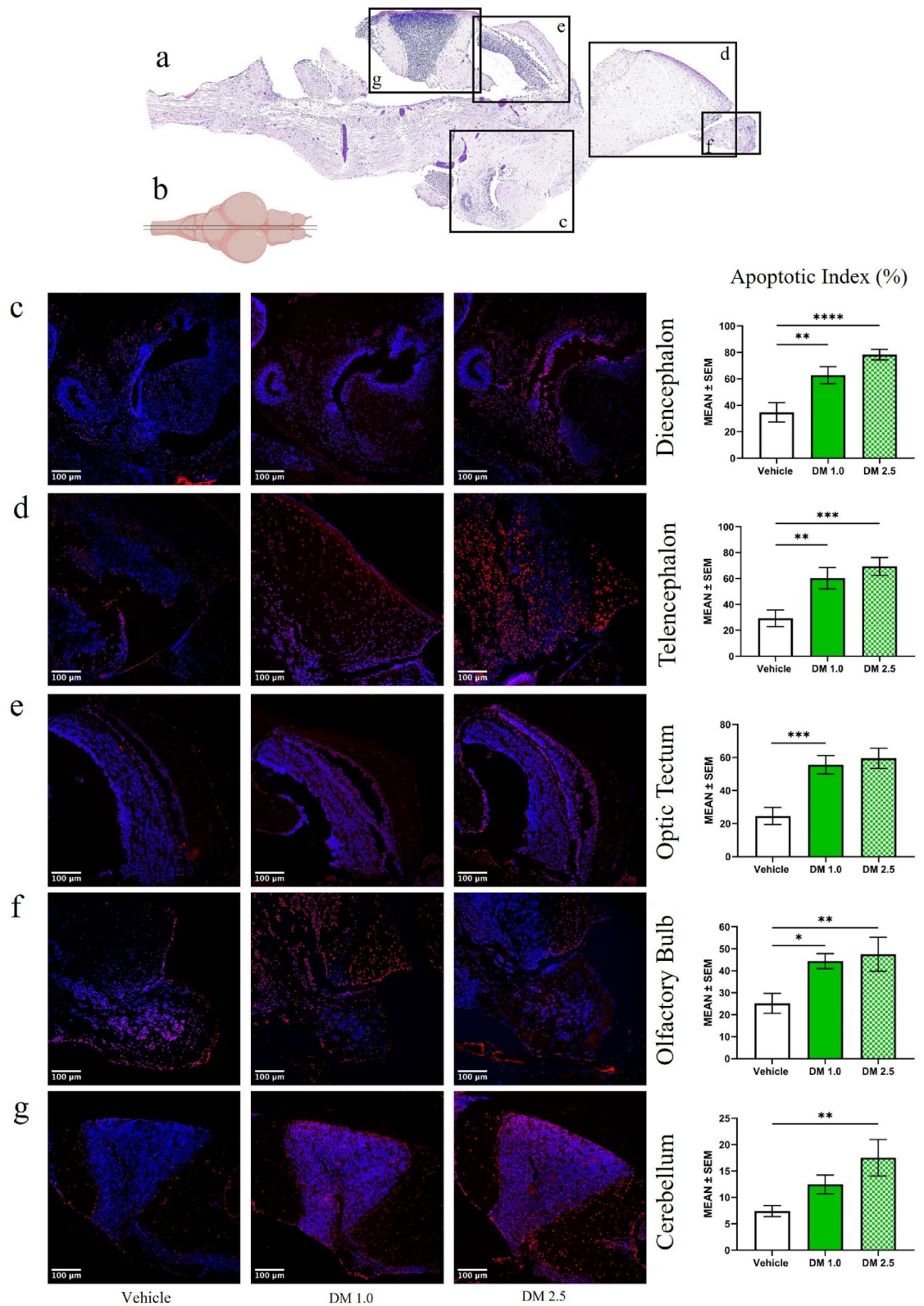


Fig. 2. TUNEL staining of brain slices of zebrafish exposed to 1.0 µg/L and 2.5 µg/L deltamethrin (DM). Hematoxylin and eosin staining of zebrafish brain highlight the zones analyzed with TUNEL staining (a). Schematic representation of zebrafish brain in dorsal view (b). Representative images of the diencephalon, telencephalon, optic tectum, olfactory bulb, and cerebellum (c-g). Nuclei are marked by DAPI (blue). Apoptotic cells are stained with TUNEL (red). From left to right, the pictures refer to the brain tissue of zebrafish exposed to the vehicle, DM 1.0 µg/L and DM 2.5 µg/L. Positive control slices are depicted in Fig. 1. On the right, data are expressed as a comparison of Apoptotic Indexes between ROT and vehicle groups. Statistical analyses were performed with one-way ANOVA, * $p < 0.05$, ** $p < 0.01$, *** $p < 0.001$, **** $p < 0.0001$.

0.451]), optic tectum (Fig. 2e, $F_{(2,44)} = 11.97, p < 0.0001, ES = 0.352, 95\% CI [0.117, 0.550]$), olfactory bulb (Fig. 2f, $F_{(2,33)} = 5.695, p = 0.0075, ES = 0.257, 95\% CI [0.024, 0.488]$), and cerebellum (Fig. 2g, $F_{(2,42)} = 4.941, p = 0.0118, ES = 0.190, 95\% CI [0.011, 0.396]$), apoptosis was significantly higher compared to the vehicle.

Multiple comparisons were based on significant main effects of the ANOVAs. The lower DM dose (1 $\mu\text{g/L}$; DM_{low}) induced apoptosis in the diencephalon ($p = 0.0043$), telencephalon ($p = 0.0076$), optic tectum ($p = 0.0005$), and olfactory bulb ($p = 0.0202$) compared to the vehicle. At the higher concentration (2.5 $\mu\text{g/L}$; DM_{high}), apoptosis was further elevated in all regions compared to the vehicle, including diencephalon ($p < 0.0001$; $DM_{\text{high}} = 78.28 \pm 3.88$; $DM_{\text{low}} = 62.79 \pm 6.21$), telencephalon ($p = 0.0004$; $DM_{\text{high}} = 69.39 \pm 6.69$; $DM_{\text{low}} = 60.25 \pm 7.96$), optic tectum ($p = 0.002$; $DM_{\text{high}} = 59.56 \pm 5.94$; $DM_{\text{low}} = 55.64 \pm 5.42$), olfactory bulb ($p = 0.0099$), and cerebellum ($p = 0.0059$). Although apoptotic index values were higher in DM_{high} than in DM_{low} in most regions, these differences did not reach statistical significance.

Similar to the ROT exposure, DM-induced cerebellum apoptotic index, although significantly higher compared to the vehicle group, was considerably smaller ($DM_{\text{high}} = 17.52 \pm 3.33$; $DM_{\text{low}} = 12.47 \pm 1.71$) compared to the other regions.

DA Cell Loss Induced by ROT Exposure

The brain regions analyzed to monitor TH-positive cells are shown in Fig. 3a, while Fig. 3b schematically indicates the site of the longitudinal brain sectioning.

ROT exposure significantly reduced TH-ir cell numbers in the posterior tuberculum (Fig. 3c; $t_{(10)} = 2.840, p = 0.0176, ES = 1.500, 95\% CI [0.264, 2.928]$) and the posterior hypothalamus (Fig. 3d; $t_{(10)} = 4.346, p = 0.0015, ES = 2.316, 95\% CI [0.910, 4.044]$). However, no significant differences were found in the preoptic area, olfactory bulbs, and pretectum compared to the vehicle; Fig. 3e-g.

DA Cell Loss Induced by DM Exposure

DM exposure induced a significant reduction in TH-ir cell number in most of the regions where DA innervation was assessed (Fig. 4a and b: schematic representation of brain sectioning). Significant cell loss was found in the posterior tuberculum (Fig. 4c; $F_{(2,15)} = 3.714, p = 0.0489, ES = 0.331, 95\% CI [0.000, 0.632]$), posterior hypothalamus (Fig. 4d; $F_{(2,15)} = 5.145, p = 0.0199, ES = 0.487, 95\% CI [0.010, 0.688]$), preoptic area (Fig. 4e; $F_{(2,13)} = 4.111, p = 0.0414, ES = 0.388, 95\% CI [0.000, 0.688]$), and pretectum (Fig. 4g; $F_{(2,15)} = 5.744, p = 0.0141, ES = 0.434, 95\% CI [0.025, 0.706]$), while in loss in the olfactory bulbs (Fig. 4f) did not reach statistical significance.

Multiple comparisons, based on significant main effects of the ANOVAs revealed that exposure to 1.0 $\mu\text{g/L}$ induced significant decrease in DA cell number in the pretectum ($p = 0.0075$), while 2.5 $\mu\text{g/L}$ induced significant damage in the posterior tuberculum ($p = 0.0296$), posterior hypothalamus ($p = 0.0111$), and preoptic area ($p = 0.0291$).

ROT-induced behavioral alterations

ROT exposure induced various behavioral alterations. Specifically, exposed animals demonstrated a shorter duration of movements at high speed (Fig. 5a, $t_{(16)} = 2.494, p = 0.0240, ES = 1.127, 95\% CI [0.153, 2.182]$) and heightened latency to enter the upper zone of the apparatus (Fig. 5d, $t_{(16)} = 2.347, p = 0.0321, ES = 1.060, 95\% CI [0.093, 2.104]$). These results indicate an alteration of locomotion and a concomitant increase in anxiety-like behavior, respectively. The alteration in locomotion is not reflected in the other parameters quantifying the zebrafish movement, such as distance moved (Fig. 5c, $t_{(16)} = 0.8585, p = 0.4033$), and absolute turn angle (Fig. 5b, $t_{(16)} = 1.956, p = 0.0681$), indicating that motor impairments were marginal. Similarly, other stress-related parameters, including the number of entries to the top (Fig. 5e, $t_{(16)} = 1.005, p = 0.3300$) and the time spent in the top (Fig. 5f, $t_{(15)} = 0.3704, p = 0.7163$), were marginally impaired. Figure 5g and h: representative images of the apparatus and vehicle (5g) or ROT-treated (5h) animal tracks during the experimental phase.

DM-induced behavioral alterations

Behavioral observations of adult zebrafish after 15-day exposure to DM revealed alterations in locomotion. The duration of swimming at high speed (Fig. 6a, $F_{(2,25)} = 4.869, p = 0.0164, ES = 0.280, 95\% CI [0.010, 0.537]$) and absolute turn angle value (Fig. 6b, $F_{(2,25)} = 3.715, p = 0.0387, ES = 0.229, 95\% CI [0.000, 0.489]$) were significantly different compared to the vehicle. As depicted in Fig. 6, only the highest DM concentration induced such significant changes in zebrafish phenotype, increasing the absolute turn angle ($p = 0.0316$) and decreasing the duration of swimming at high speed ($p = 0.0100$), suggesting that the exposure affected the locomotion without impacting anxiety-like behavior parameters, even though the distance moved (Fig. 6c, $F_{(2,25)} = 1.439, p = 0.2562$) was not impacted. In fact, the latency to the top (Fig. 6d, $F_{(2,25)} = 1.803, p = 0.1856$), the number of transitions to the top (Fig. 6e, $F_{(2,25)} = 0.08717, p = 0.9168$), and time spent in the top (Fig. 6f, $F_{(2,24)} = 0.6535, p = 0.5292$) did not show any difference between the vehicle and the DM-treated fish although the pattern of activity, as shown by the representative animal tracks resulted altered (Fig. 6g-i).

Summary

An infographic table is illustrated below. It summarizes all the results obtained in the present study. The p -values of the single findings are reported for all experiments. Table 1

Discussion

Pesticides are frequently used in agriculture to enhance crop production, although their improper and extensive application leads to environmental contamination^{1,43}. The widespread consumption of pesticides such as ROT and DM raises significant concerns about their adverse effects on aquatic fauna and broader ecological systems. These adverse effects include neurological and behavioral disorders, which have been documented

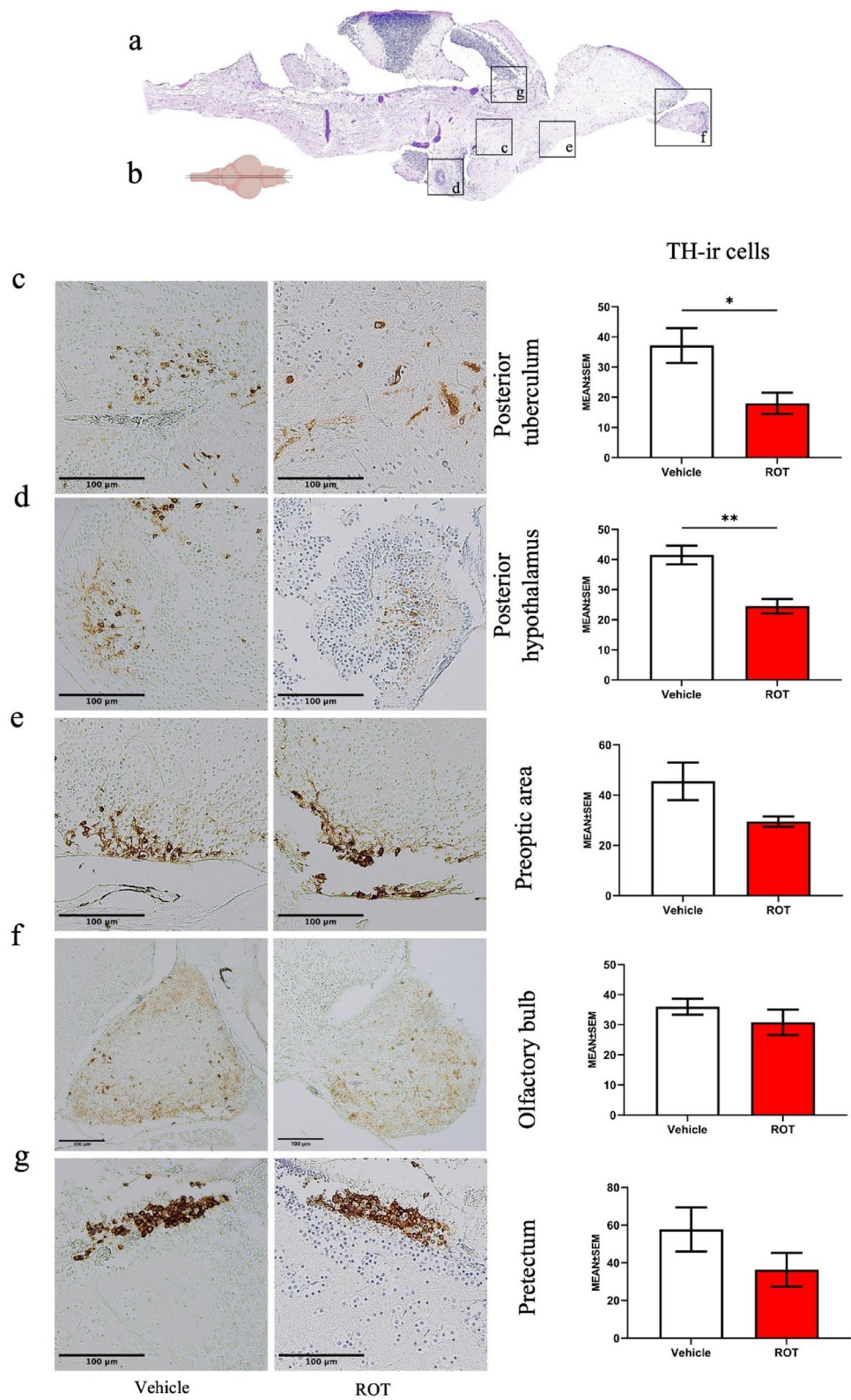


Fig. 3. Quantification of TH-ir cells in discrete regions of the zebrafish brain involved in DA transmission in zebrafish exposed to 2.0 µg/L ROT. Hematoxylin and eosin staining of a zebrafish brain highlight the zones analyzed by the IHC staining of TH-ir neurons (a). Schematic representation of zebrafish brain in dorsal view (b). Representative images of the posterior tuberculum, posterior hypothalamus, preoptic area, olfactory bulbs, and preteectum (c-g). Nuclei are marked by hematoxylin (blue), TH-ir cells are stained in IHC with HRP-DAB reaction (brown). From left to right, the pictures refer to the brain tissue of zebrafish exposed to the vehicle and ROT. On the right, data are expressed as a comparison of the number of TH-ir cells between ROT and vehicle group. Statistical analyses were performed with Student’s t-test, * $p < 0.05$, ** $p < 0.01$.

in adult zebrafish, a widely recognized vertebrate model for analyzing the toxicity of environmental chemical substances⁴⁴. The present study confirmed that chronic exposure to both ROT and DM is neurotoxic to zebrafish, leading to profound neuronal cell death and behavioral changes. Furthermore, studies on the side effects of ROT exposure in humans suggest that individuals with frequent use rotenone have a 2.5-fold higher risk of developing Parkinson's disease (PD), even when exposure occurred years before symptom onset^{45,46}.

TUNEL assay revealed that the most susceptible brain regions exposed to ROT were the diencephalon, optic tectum, and cerebellum, exhibiting a significant increase in apoptotic index, as compared to the vehicle. Among the affected regions, the diencephalon exhibited the highest level of apoptosis, consistent with the posterior tuberculum, a crucial region that sends ascending projections to the subpallium (SP), which are thought to serve functions analogous to the mesodiencephalic dopamine systems in mammals⁴⁷. The pronounced apoptosis in this region further supports previous studies demonstrating the vulnerability of DA neurons to ROT-induced oxidative stress and mitochondrial dysfunction^{17,48}. Additionally, the optic tectum and cerebellum also show considerable apoptotic activity, suggesting a broader neurotoxic impact of chronic ROT exposure in regions associated with sensory processing and motor coordination.

Furthermore, ROT significantly reduced the number of DA neurons in the posterior tuberculum and posterior hypothalamus, demonstrating the disruptive effect of ROT in regions related to movement regulation. The role of the posterior tuberculum in zebrafish movement parallels the function of the substantia nigra in humans, which regulates movement through DA signaling^{49–51}. Recent studies confirmed that ROT exposure in zebrafish induces PD-like symptoms, including motor deficits, DA neuron loss, and oxidative stress, consistent with the neurodegenerative processes observed in PD^{17,52}. Similarly, in rodent models, ROT exposure impairs movements and coordination, along with DA neuron loss and α -synuclein aggregation in the brain, particularly in the substantia nigra, which is critically involved in PD pathogenesis⁵³. Likewise, Liu and colleagues showed that chronic exposure to ROT caused significant motor impairment and DA depletion in mice striatum⁵⁴. These findings highlight the ecological risks posed by rotenone, a widely used pesticide and piscicide, which, through the neurotoxic effects, can impair neurological function and survival in aquatic species. In addition, the use in aquatic environments not only targets invasive fish but also adversely affects non-target organisms, including sensitive invertebrate taxa, potentially disrupting community structure and ecosystem balance⁵⁵. Given the conserved nature of dopaminergic systems across vertebrates, such exposure may have broader implications for wildlife health and biodiversity, emphasizing the need for careful environmental monitoring and management strategies to mitigate rotenone's ecological impact.

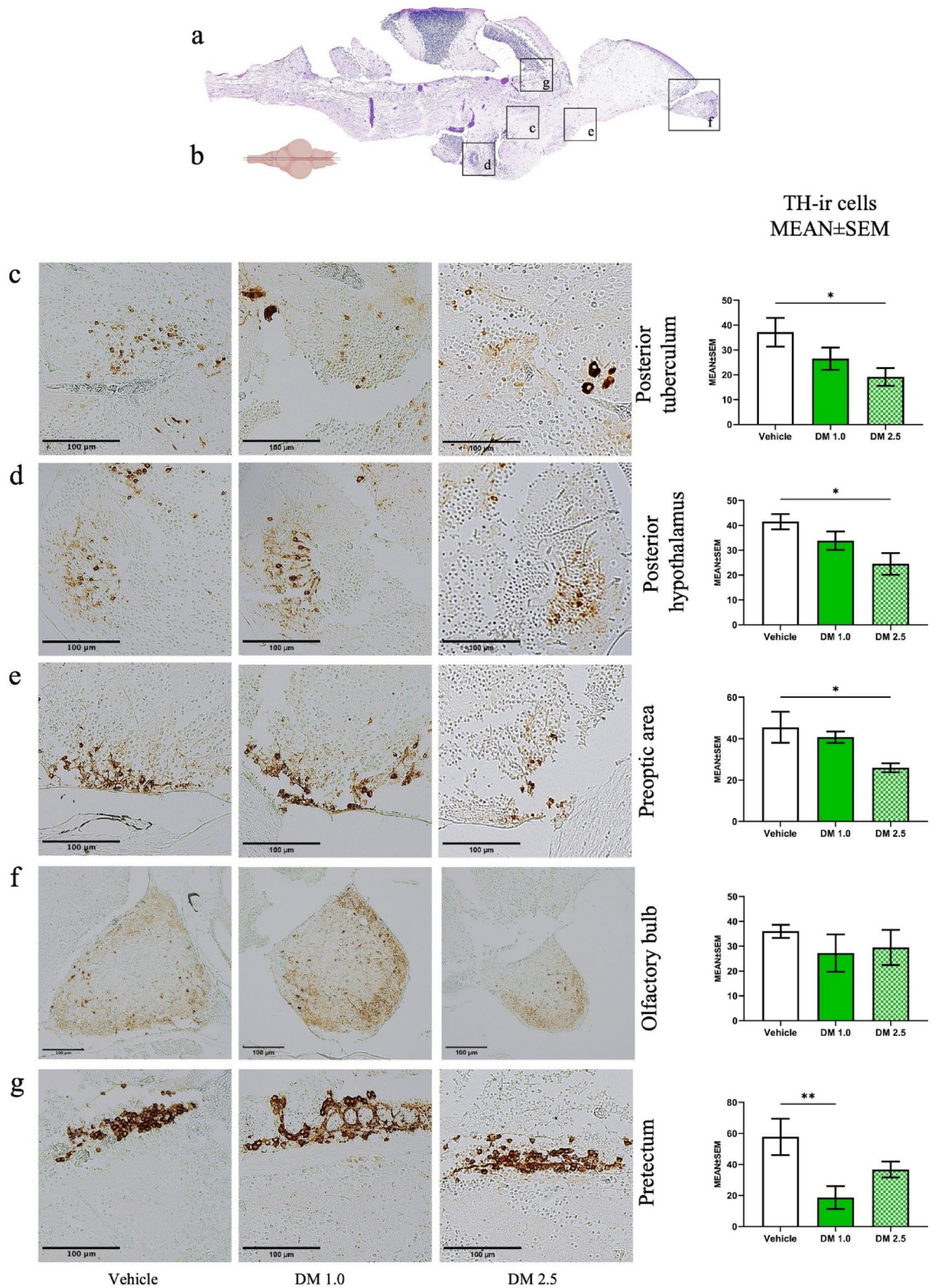
The behavioral findings align with the literature, demonstrating a significant reduction in the duration of high-speed movements, but also uncovered stress-like behaviors in ROT-exposed fish^{17,54}. DM concentrations of 1 and 2.5 $\mu\text{g/L}$ were chosen to represent levels observed in aquatic ecosystems, which typically range from 0.04 $\mu\text{g/L}$ to 24 $\mu\text{g/L}$ in agricultural regions where this pesticide is employed⁵⁶. DM chronic exposure induced apoptosis in several zebrafish brain regions, including the diencephalon, telencephalon, and optic tectum.

DM exposure significantly induced DA cell loss across various brain regions in a dose-dependent manner. At 1.0 $\mu\text{g/L}$, damage was confined to the pretectum, while 2.5 $\mu\text{g/L}$ exposure led to broader effects in the posterior tuberculum, posterior hypothalamus, and preoptic area. In agreement with our findings, previous studies showed that developmental exposure to DM caused alterations in larval DA neurochemistry and gene expression, increased levels of HVA, and decreased levels of the *drd1* and *drd2a* transcripts⁵⁷. In addition, DM intranasal exposure in rats induced reduction in TH-immunoreactive neurons in the substantia nigra pars compacta and ventral tegmental area, identifying DM damage as a potential risk factor for PD⁵⁸.

Also behavioral assays revealed significant locomotion impairments, mainly following DM_{high} exposure. The increased absolute turn angle and reduced duration of high-speed swimming suggest impaired motor coordination. These behavioral changes likely stem from the combined effects of apoptotic cell death and DA dysfunction. Additionally, fish exhibited anxiety-like behavior characterized by erratic movements and irregular movements.

Lei and colleagues found that fish exposed to 100 ng/L DM exhibited significantly decreased nearest-neighbor distance (NND) and inter-individual distance (IID) during the shoaling test⁵⁹, suggesting heightened stress/anxiety-like behavior in treated animals, as stressed fish tend to swim in closer proximity to one another⁶⁰. Moreover, it has been reported that chronic exposure to DM at concentrations of 0.5 $\mu\text{g/L}$ induced aggressive behavior and neurological disorders. Furthermore, when the concentration doubled, an alternation between aggressive and non-aggressive behavior was observed, suggesting high cognitive damage²¹.

The combined observation of histological and behavioral impairments provides critical insights for ecological risk assessment in aquatic ecosystems. Histological damage directly reflects the cellular and tissue-level toxicity of these compounds, while behavioral changes demonstrate functional impairments that can affect survival^{59,61}. Integrating these endpoints allows for a more comprehensive evaluation of sublethal effects that may not be immediately lethal but can disrupt population dynamics and ecosystem stability. From a risk assessment perspective, these findings support the need to establish environmental guidelines that consider both neurotoxic and reproductive endpoints, also at environmentally subthreshold concentrations⁸. Specifically, regulatory frameworks should incorporate chronic exposure limits that prevent histopathological damage and behavioral dysfunction in non-target aquatic species. Moreover, the evidence of dopaminergic disruption highlights the importance of monitoring biomarkers linked to neurotoxicity in environmental exposure studies. Future studies should focus on the long-term effects of combined pesticide exposures, as well as their impacts on ecological behaviors such as predator avoidance, mating, and social interactions. Despite valuable insights gained from this study, it lacks the evaluation of genes involved in dopamine synthesis or transporters. Additionally, assessing pro-inflammatory markers and oxidative stress factors would provide a more comprehensive understanding of the neurological alterations.



Conclusions

Synthetic chemical pesticides are crucial in agriculture to prevent pests and weeds from ravaging crops. However, they can harm unintended animals and plants and leach into surrounding waterways and soil, expanding their toxic reach. This study underscores the significant impacts of chronic ROT and DM exposure on apoptosis, DA neuronal integrity, and behavior in adult zebrafish, highlighting the need to address pesticide contamination in aquatic environments.

Our study contributes to the broader understanding of how chronic pesticide exposure affects aquatic vertebrates, providing a basis for further research into the long-term ecological and health implications. The use

Fig. 4. Quantification of TH-ir cells in discrete regions of the zebrafish brain involved in DA transmission in zebrafish exposed to 1.0 and 2.5 $\mu\text{g/L}$ deltamethrin (DM). Hematoxylin and eosin staining of a zebrafish brain highlight the zones analyzed by the IHC staining of TH-ir neurons (a). Schematic representation of zebrafish brain in dorsal view (b). Representative images of the posterior tuberculum, posterior hypothalamus, preoptic area, olfactory bulbs, and pretectum (c-g). Nuclei are marked by hematoxylin (blue), and TH-ir cells are stained in IHC with HRP-DAB reaction (brown). From left to right, the pictures refer to the brain tissue of zebrafish exposed to the vehicle, DM 1.0 $\mu\text{g/L}$ and DM 2.5 $\mu\text{g/L}$. On the right, data are expressed as a comparison of the number of TH-ir cells between the DM 1.0 $\mu\text{g/L}$, DM 2.5 $\mu\text{g/L}$, and vehicle groups. Statistical analyses were performed with one-way ANOVA, * $p < 0.05$, ** $p < 0.01$.

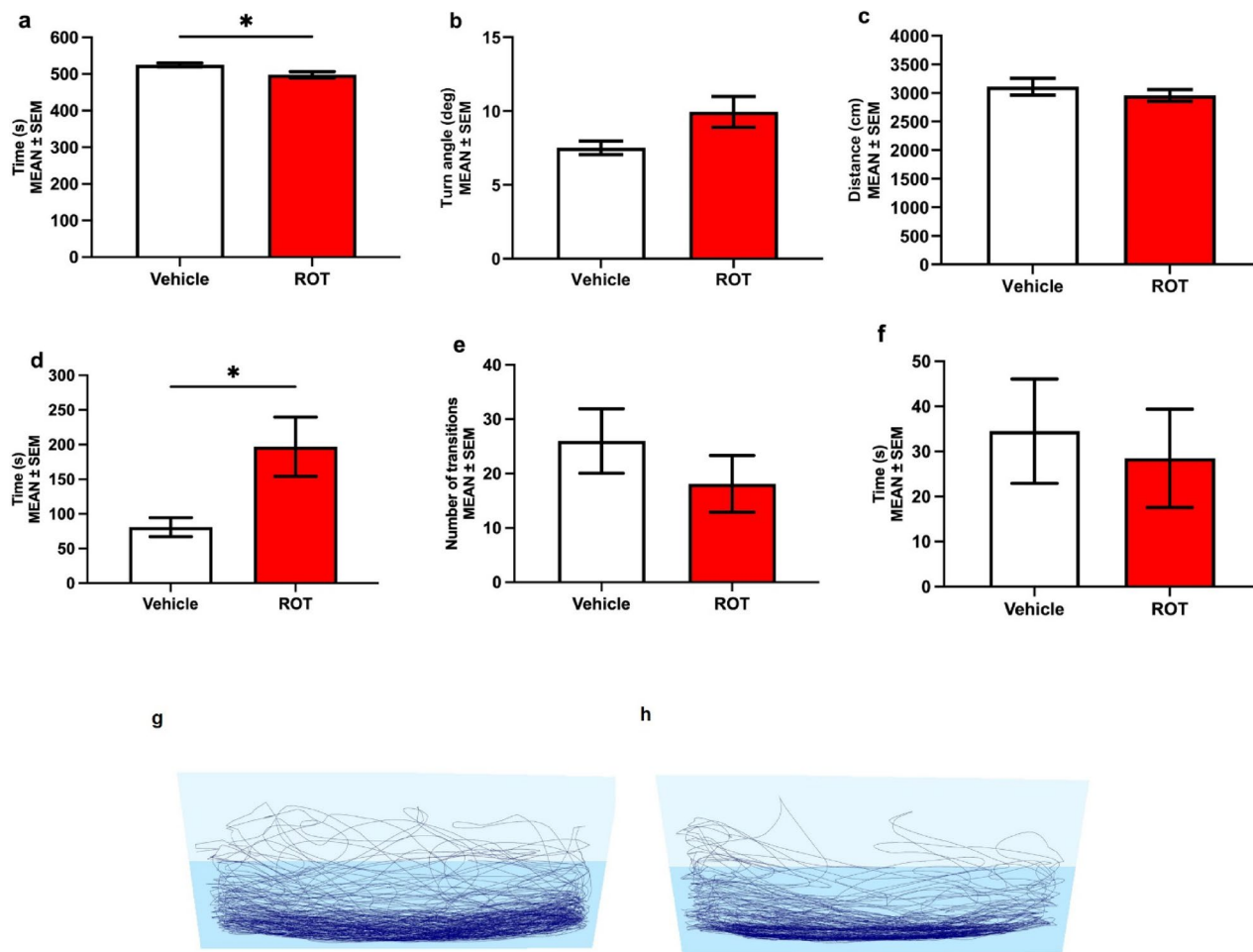


Fig. 5. Novel tank test results after ROT exposure. On the top, data are expressed as a comparison between ROT and vehicle groups (a-f). Duration of swimming at high speed (a); Absolute turn angle (b); Distance moved (c); Latency to enter the top zone (d); Number of entries to the top zone (e), and Time in the top zone (f). Representative images of the apparatus and animal tracks during the experimental phase (g-h). Vehicle (g); ROT (h). Statistical analyses were performed using Student's *t*-test, * $p < 0.05$.

of zebrafish as a model organism proved effective in elucidating the behavioral and neuronal impacts of these pesticides, supporting their relevance in environmental toxicology studies.

Our findings reveal that both ROT and DM induce apoptosis in specific brain regions, with ROT predominantly affecting the diencephalon, optic tectum, and cerebellum, while DM prevalently affecting the diencephalon, telencephalon, and optic tectum. Additionally, both pesticides significantly reduced DA neuron density, with ROT targeting the posterior tuberculum and posterior hypothalamus and DM exhibiting broader DA depletion at higher concentrations. The neurotoxic effects of ROT parallel mechanisms observed in Parkinson's disease. In the Novel Tank Test, the primary observations relate to motor impairments rather than traditional anxiety-

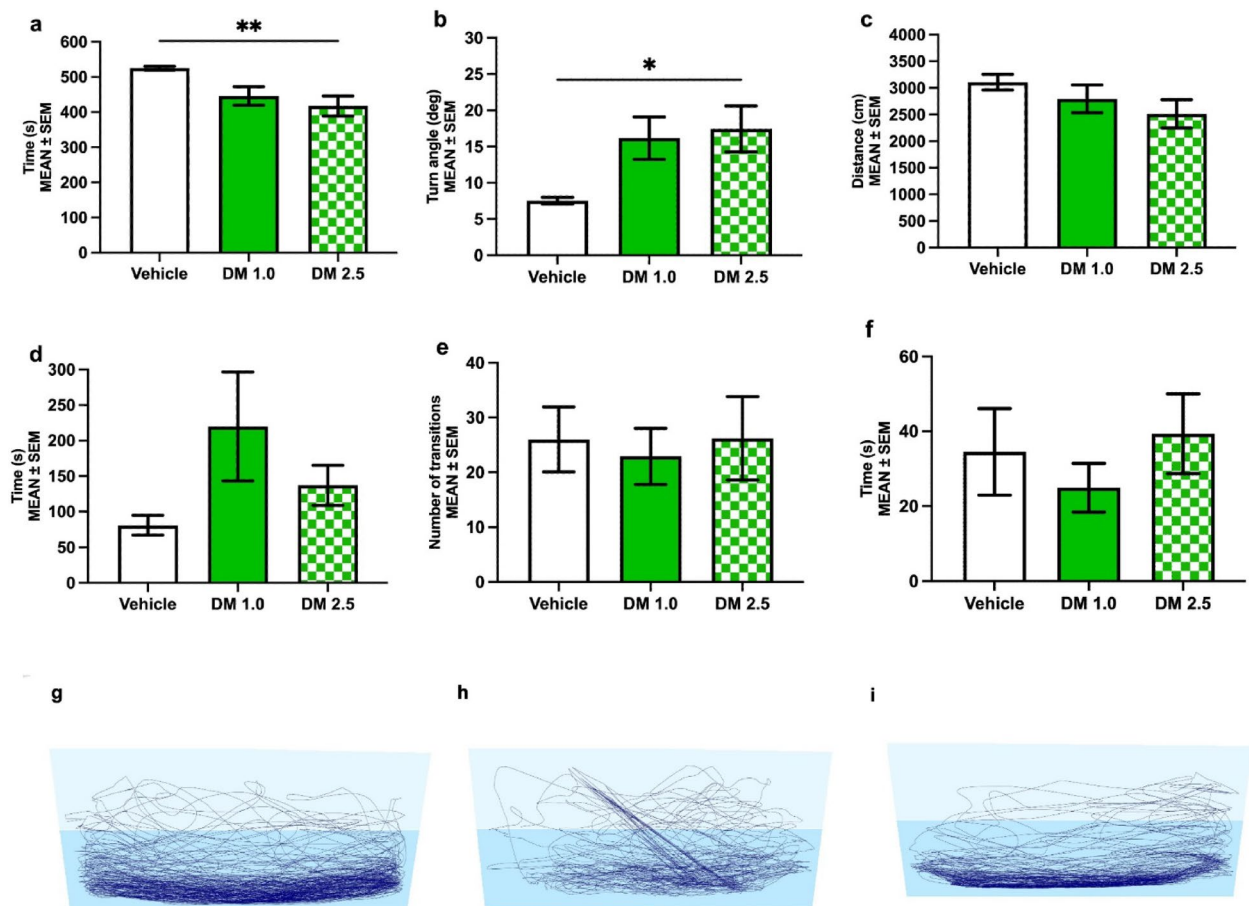


Fig. 6. Novel tank test results after DM exposure. On the top, data are expressed as comparisons between the DM and vehicle groups (a–f). Duration of swimming at high speed (a); Absolute turn angle (b); Distance moved (c); Latency to enter the top zone (d); Number of entries to the top zone (e) and Time in the top zone (f). Representative images of the apparatus and animal tracks during the experimental phase (g–i). Vehicle (g); DM 1.0 $\mu\text{g/L}$ (h); I. DM 2.5 $\mu\text{g/L}$ (i). Statistical analyses were performed using one-way ANOVA, $*p < 0.05$, $**p < 0.01$.

like measures such as time spent in the top zones and number of entries. This could be due to the involvement of dopaminergic neurotransmission, which is strongly damaged by the pesticide exposure, and is crucial for motor coordination. Further studies focusing on stress-related behaviors and anxiety-like outcomes, rather than locomotion, might help to better understand stress-specific consequences. Behavioral assessments demonstrated that exposure to both pesticides impaired motor coordination and induced anxiety-like behaviors, emphasizing the intricate interconnections between neural cellular/circuit damage and behavioral alterations.

Data availability

Data availability Data is provided within the manuscript.

Received: 26 March 2025; Accepted: 23 July 2025

Published online: 25 July 2025

References

- Wang, F. et al. Emerging contaminants: A one health perspective. *Innov.* **5**, 100612 (2024).
- Tudi, M. et al. Agriculture development, pesticide application and its impact on the environment. *IJERPH* **18**, 1112 (2021).
- ISPRA. *National report on pesticides in waters 2022 edition (2019–2020 data)*. 371/ ISPRA, (2022). https://www.isprambiente.gov.it/files2022/publicazioni/rapporti/rapporto_371_2022.pdf (2022, accessed 8 February 2024).
- Cosgrove, S., Jefferson, B. & Jarvis, P. Pesticide removal from drinking water sources by adsorption: a review. *Environ. Technol. Reviews*. **8**, 1–24 (2019).
- Mojiri, A. et al. Pesticides in aquatic environments and their removal by adsorption methods. *Chemosphere* **253**, 126646 (2020).
- Arisekar, U. et al. Accumulation of organochlorine and pyrethroid pesticide residues in fish, water, and sediments in the Thamirabarani river system of Southern Peninsular India. *Environ. Nanotechnol. Monit. Manage.* **11**, 100194 (2019).

7. Shamsollahi, Z. & Partovinia, A. Recent advances on pollutants removal by rice husk as a bio-based adsorbent: A critical review. *J. Environ. Manage.* **246**, 314–323 (2019).
8. Lunghi, C. et al. Call to action: pharmaceutical residues in the environment: threats to ecosystems and human health. *Drug Saf* **48**, 315–320 (2024)
9. Richardson, J. R. et al. Neurotoxicity of pesticides. *Acta Neuropathol.* **138**, 343–362 (2019).
10. Vellingiri, B. et al. Neurotoxicity of pesticides – A link to neurodegeneration. *Ecotoxicol. Environ. Saf.* **243**, 113972 (2022).
11. Gupta, R. C. & Milatovic, D. Insecticides. In: *Biomarkers in Toxicology*. Elsevier, pp. 389–407 (2014).
12. Nandipati, S. & Litvan, I. Environmental exposures and parkinson's disease. *Int. J. Environ. Res. Public Health.* **13**, 881 (2016).
13. Xiong, N. et al. Mitochondrial complex I inhibitor rotenone-induced toxicity and its potential mechanisms in parkinson's disease models. *Crit. Rev. Toxicol.* **42**, 613–632 (2012).
14. Cannon, J. R. & Greenamyre, J. T. Neurotoxic in vivo models of Parkinson's disease. pp. 17–33. (2010).
15. Betarbet, R. et al. Chronic systemic pesticide exposure reproduces features of parkinson's disease. *Nat. Neurosci.* **3**, 1301–1306 (2000).
16. Robea, M.-A. et al. Parkinson's Disease-Induced Zebrafish Models: Focussing on Oxidative Stress Implications and Sleep Processes. *Oxidative Medicine and Cellular Longevity*; 2020: 1–15. (2020).
17. Wang, Y. et al. Parkinson's disease-like motor and non-motor symptoms in rotenone-treated zebrafish. *Neurotoxicology* **58**, 103–109 (2017).
18. Daubner, S. C., Le, T. & Wang, S. Tyrosine hydroxylase and regulation of dopamine synthesis. *Arch. Biochem. Biophys.* **508**, 1–12 (2011).
19. Wasel, O. & Freeman, J. L. Chemical and genetic zebrafish models to define mechanisms of and treatments for dopaminergic neurodegeneration. *Int. J. Mol. Sci.* **21**, 5981 (2020).
20. Bretaud, S., Lee, S. & Guo, S. Sensitivity of zebrafish to environmental toxins implicated in parkinson's disease. *Neurotoxicol. Teratol.* **26**, 857–864 (2004).
21. Strungaru, S.-A. et al. Toxicity and chronic effects of deltamethrin exposure on zebrafish (*Danio rerio*) as a reference model for freshwater fish community. *Ecotoxicol. Environ. Saf.* **171**, 854–862 (2019).
22. Wu, X. et al. Biological removal of deltamethrin in contaminated water, soils and vegetables by *Stenotrophomonas maltophilia* XQ08. *Chemosphere*; 279: 130622. (2021).
23. Toumi, H. et al. Effect of deltamethrin (pyrethroid insecticide) on two clones of daphnia magna (Crustacea, Cladocera): A proteomic investigation. *Aquat. Toxicol.* **148**, 40–47 (2014).
24. Johnson, M. et al. Deltamethrin Technical Fact Sheet, (2010). <https://npic.orst.edu/factsheets/archive/Deltatech.html>. accessed 10 January 2025).
25. Pitzer, E. M., Williams, M. T. & Vorhees, C. V. Effects of pyrethroids on brain development and behavior: deltamethrin. *Neurotoxicol. Teratol.* **87**, 106983 (2021).
26. Magendira Mani, V., Asha, S. & Sadiq, A. M. M. Pyrethroid deltamethrin-induced developmental neurodegenerative cerebral injury and ameliorating effect of dietary glycoside naringin in male Wistar rats. *Biomed. Aging Pathol.* **4**, 1–8 (2014).
27. USEPA/Office of Pesticide Programs. Reregistration Eligibility Decision Document - Rotenone p.10 EPA 738-R-07-005 (March 2007), (2007). https://www3.epa.gov/pesticides/chem_search/reg_actions/reregistration/red_PC-071003_31-Mar-07.pdf accessed 19 May 2025).
28. Sandodden, R. et al. Rotenone application and degradation following eradication of invasive Roach (*Rutilus rutilus*) in three Norwegian lakes. *MBI* **13**, 233–245 (2022).
29. Rodrigues, S. et al. Assessment of the ecotoxicological effects of deltamethrin to daphnia magna: linking sub-individual and supra-individual parameters. *Watershed Ecol. Environ.* **5**, 231–240 (2023).
30. SCHEER (Scientific Committee on Health, Environmental and Emerging Risks). Final Opinion on Draft Environmental Quality Standards for Priority Substances under the Water Framework Directive - Deltamethrin, https://health.ec.europa.eu/publications/draft-environmental-quality-standards-priority-substances-under-water-framework-directive-1_en (2022). accessed 19 May 2025).
31. Meléndez, J. L. et al. Risks of Deltamethrin Use to Federally Threatened, https://search.epa.gov/epasearch/?querytext=deltamethrin&areaname=&areacontacts=&areasearchurl=&typeofsearch=epa&result_template=#/ accessed 19 May 2025).
32. Horzmann, K. & Freeman, J. Zebrafish get connected: investigating neurotransmission targets and alterations in chemical toxicity. *Toxics* **4**, 19 (2016).
33. Lin, Q. & Jesuthasan, S. Masking of a circadian behavior in larval zebrafish involves the thalamo-habenula pathway. *Sci. Rep.* **7**, 4104 (2017).
34. Mueller, T. What is the thalamus in zebrafish?? *Front. Neurosci.* **6** <https://doi.org/10.3389/fnins.2012.00064> (2012). Epub ahead of print.
35. Wullimann, M. F., Rupp, B. & Reichert, H. Epub ahead of print 1996. In *Neuroanatomy of the Zebrafish Brain* (Birkhäuser Basel, 1996). <https://doi.org/10.1007/978-3-0348-8979-7>.
36. Pietsch, C. et al. Multiple faces of stress in the zebrafish (*Danio rerio*) brain. *Front. Physiol.* **15**, 1373234 (2024).
37. Fuzzen, M. L. M., Van Der Kraak, G. & Bernier, N. J. Stirring up new ideas about the regulation of the Hypothalamic-Pituitary-Interrrenal axis in zebrafish (*Danio rerio*). *Zebrafish* **7**, 349–358 (2010).
38. Buzenchi Proca, T. M., Solcan, C. & Solcan, G. Neurotoxicity of some environmental pollutants to zebrafish. *Life* **14**, 640 (2024).
39. Vaz, R., Hofmeister, W. & Lindstrand, A. Zebrafish models of neurodevelopmental disorders: limitations and benefits of current tools and techniques. *IJMS* **20**, 1296 (2019).
40. Copper, J. E. et al. Comparative analysis of fixation and embedding techniques for optimized histological Preparation of zebrafish. *Comp. Biochem. Physiol. C: Toxicol. Pharmacol.* **208**, 38–46 (2018).
41. Kenney, J. W. et al. A 3D adult zebrafish brain atlas (AZBA) for the digital age. *eLife*; 10. Epub ahead of print 22 November 2021. <https://doi.org/10.7554/eLife.69988>
42. Greenwald, A. G. et al. Effect sizes and p values: what should be reported and what should be replicated? *Psychophysiology* **33**, 175–183 (1996).
43. Badruzzaman, M. et al. Rotenone alters behavior and reproductive functions of freshwater catfish, *Mystus cavasius*, through deficits of dopaminergic neurons in the brain. *Chemosphere* **263**, 128355 (2021).
44. Kari, G., Rodeck, U. & Dicker, A. P. Zebrafish: an emerging model system for human disease and drug discovery. *Clin. Pharmacol. Ther.* **82**, 70–80 (2007).
45. Kamel, F. Paths from pesticides to parkinson's. *Science* **341**, 722–723 (2013).
46. Tanner, C. M. et al. Rotenone, paraquat, and parkinson's disease. *Environ. Health Perspect.* **119**, 866–872 (2011).
47. Tay, T. L. et al. Comprehensive catecholaminergic projectome analysis reveals single-neuron integration of zebrafish ascending and descending dopaminergic systems. *Nat. Commun.* **2**, 171 (2011).
48. Nies, Y. H. et al. Metallothionein II treatment mitigates rotenone-induced neurodegeneration in zebrafish models of parkinson's disease. *Front. Pharmacol.* **16**, 1478013 (2025).
49. Paolone, G. From the gut to the brain and back: therapeutic approaches for the treatment of network dysfunction in parkinson's disease. *Front. Neurol.* **11**, 557928 (2020).
50. Paolone, G. et al. Eltopazine prevents levodopa-induced dyskinesias by reducing striatal glutamate and direct pathway activity. *Mov. Disord.* **30**, 1728–1738 (2015).

51. Kucinski, A. et al. Modeling fall propensity in parkinson's disease: deficits in the attentional control of complex movements in rats with Cortical-Cholinergic and Striatal-Dopaminergic deafferentation. *J. Neurosci.* **33**, 16522–16539 (2013).
52. Nies, Y. H. et al. Microarray-based analysis of differential gene expression profile in Rotenone-induced parkinson's disease zebrafish model. *CNSNDDT* **23**, 761–772 (2024).
53. Innos, J. & Hickey, M. A. Using rotenone to model parkinson's disease in mice: A review of the role of pharmacokinetics. *Chem. Res. Toxicol.* **34**, 1223–1239 (2021).
54. Liu, Y. et al. Environment-contact administration of rotenone: A new rodent model of parkinson's disease. *Behav. Brain. Res.* **294**, 149–161 (2015).
55. Dalu, T. et al. An assessment of the effect of rotenone on selected Non-Target aquatic fauna. *PLoS ONE.* **10**, e0142140 (2015).
56. Pawlisz, A. V. et al. Canadian water quality guidelines for deltamethrin. *Environ. Toxicol. Water. Qual.* **13**, 175–210 (1998).
57. Kung, T. S. et al. Developmental deltamethrin exposure causes persistent changes in dopaminergic gene expression, neurochemistry, and locomotor activity in zebrafish. *Toxicol. Sci.* **146**, 235–243 (2015).
58. Souza, M. F. et al. Deltamethrin intranasal administration induces memory, emotional and tyrosine hydroxylase immunoreactivity alterations in rats. *Brain Res. Bull.* **142**, 297–303 (2018).
59. Lei, L. et al. New evidence for neurobehavioral toxicity of deltamethrin at environmentally relevant levels in zebrafish. *Sci. Total Environ.* **822**, 153623 (2022).
60. Nunes, A. R. et al. Social Phenotypes in Zebrafish. In *The rights and wrongs of zebrafish: Behavioral phenotyping of zebrafish* (eds Kalueff, A. V. et al.) (Springer International Publishing), 95–130 (2017).
61. Ilie, O.-D. et al. Assessing Anti-Social and aggressive behavior in a zebrafish (*Danio rerio*) model of parkinson's disease chronically exposed to rotenone. *Brain Sci.* **12**, 898 (2022).

Acknowledgements

The authors are thankful to the University Laboratory for Medical Research (LURM) and the Neuropathology Laboratory at the University of Verona for providing technical support and access to the facilities throughout the project.

Author contributions

Jacopo Grisotto, Shima Tavakolian Haghghi, Atena Poor Sasan, and Serena Pedron performed material preparation, data collection, and analysis. Jacopo Grisotto and Shima Tavakolian Haghghi wrote the first draft of the manuscript, Matteo Brunelli provided special contribution with histological investigations, Ugo Moretti has made substantial contributions to the concept and design of the study, Giovanna Paolone conceived the original idea, significantly contributed to the writing, and provided constant support during manuscript production. All data generated during this study are included in this published article and its supplementary information files.

Declarations

Competing interests

The authors declare no competing interests.

Additional information

Correspondence and requests for materials should be addressed to G.P.

Reprints and permissions information is available at www.nature.com/reprints.

Publisher's note Springer Nature remains neutral with regard to jurisdictional claims in published maps and institutional affiliations.

Open Access This article is licensed under a Creative Commons Attribution-NonCommercial-NoDerivatives 4.0 International License, which permits any non-commercial use, sharing, distribution and reproduction in any medium or format, as long as you give appropriate credit to the original author(s) and the source, provide a link to the Creative Commons licence, and indicate if you modified the licensed material. You do not have permission under this licence to share adapted material derived from this article or parts of it. The images or other third party material in this article are included in the article's Creative Commons licence, unless indicated otherwise in a credit line to the material. If material is not included in the article's Creative Commons licence and your intended use is not permitted by statutory regulation or exceeds the permitted use, you will need to obtain permission directly from the copyright holder. To view a copy of this licence, visit <http://creativecommons.org/licenses/by-nc-nd/4.0/>.

© The Author(s) 2025